Temperature Field Distribution Analysis of Electrical Contacts for High-current Equipment

Dusan Medved
Department of Electric Power Engineering
Technical University in Kosice
Kosice, Slovakia
Dusan.Medved@tuke.sk

***Abstract*—This paper deals with the analysis of contacts for high-current equipment. The issue of electrical contacts is an area in which the tasks of solving material, mechanical, electrical and last, but not least, temperature relations describing the processes of electrical current transfer through contacts meet. Knowing the exact distribution of the temperature field of and around the electrical contacts allows manufacturers to select the right material, resize the shape, or adjust the conductive path so that the electrical contact does not overheat and perform the function of the re-switching element in the electrical circuit.**

Keywords—temperature field, electrical contact, ANSYS, high-current equipment

I. Introduction

Each electrical switchgear shall have a current path so arranged that it can be interrupted at one point during the operation. The intersection point, but also the path of interconnection, has some different characteristics from the other sections. The conductive connection of the two separated parts of the flow path is realized by means of contacts.

The interruption of the electric current path can be performed under various operating conditions, e.g. with current, without current, at different voltages, with high switching frequency and other. This fact places contacts between important parts of the devices. Nowadays, high demands are placed on contacts and therefore they deserve considerable attention. In general, the requirements for contacts can be characterized as follows [1]:

- low contact resistance,
- high resistance to mechanical attrition (mainly against contact friction),
- high resistance to welding,
- high resistance to electric arc,
- optimum effect on the development of deionization processes after extinguishing of breaking arc (good switching ability).

II. Characteristics of Selected Saddle Electrical Contact

A. High-current saddle electric contacts for 250 ÷ 3000 A

The selected type of saddle contacts has several applications and therefore several advantages.

This type of contacts if offered for decades and technically is up-to-date and continuously still under development. It is supplied either as one piece standard contact for a bus-bar thickness of 10/15 or 20 mm or as a ready-to-install contact unit complete with base, i.e., integrated power connection bar or angle and insulation plate. Contacts with base are suitable for immediate installation on the tank frame. In order to maximize the life-span of the contacts and to minimize the repair and down times it is recommended to use protective covers. Protective covers used in heavy-duty applications also have an integrated 10 mm stainless steel mounting guide and are recommended especially when using heavier bus-bars. The mounting guide catches the bar securely making it easy to position properly. If someone want to use the normal protective cover or no cover, an alternative is to install a mounting guide made of red brass, afterwards. This type of contact saddles provide the following advantages and enable the least amount of current loss to the bus-bars and tank contents when the system is planned and utilized professionally.

B. Main advantages and construction features

- Self-tightening: Insertion of bars using their own weight and therefore suitable for fully automatic system operation.
- Self-cleaning: Contact surfaces are rubbed clean while the bars are inserted.
- Conductivity: Contact saddles and foil package are made of E-Cu with guaranteed conductivity.
- Robust: Stable work rod construction made of red bronze as well as stainless steel protective cover.
- Compact: Minimal installation area even for high current.
- Maintenance Friendly: Simple exchange of individual parts. Produced according to modular principle. Complete replacement contact elements or individual foils can be simply exchanged

Fig. 1. View on the standard saddle electrical contacts

978-1-7281-4358-3/19/$31.00 ©2019 IEEE

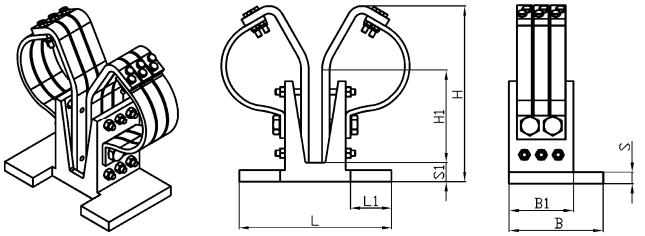

Fig. 2. View on the standard saddle contact a) spatial view; b) front view; c) side view

TABLE I. VALUES OF MAXIMAL LOAD AND PARTICULAR DIMENSIONS OF CONTACTS

		Dimensions (mm)							
Max. load (A)	Number of contact fingers 15×8 (mm)	L	L1	B	B1	H	H1	S	S1
250	4	160	35	75	45	150	60	10	20
500	6	160	40	95	65	150	60	12	20
1000	6	160	40	95	65	150	60	12	20
1500	6	160	40	95	65	150	60	12	20
2000	8	160	40	80		180	85	12	20
2500	10	195	50	100		180	85	14	20
3000	14	230	55	135		180	85	16	20

III. TEMPERATURE FIELD DISTRIBUTION OF 500 A ELECTRICAL CONTACT

Based on the presented Table 1, an analysis of the suitability of using a saddle contact for 500 A application was performed, with the condition of not exceeding 75 °C at any point of contact as well as bus-bar being chosen as the main parameter.

As an example of thermal field distribution calculation, a 500 A saddle electrical contact was chosen, which is variable and some of its dimensional or material parameters can be modified according to the manufacturer.

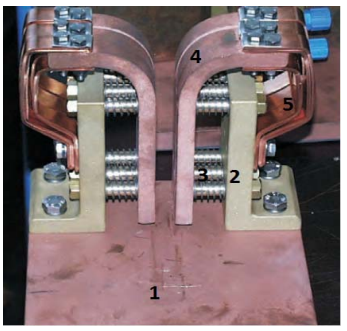

Fig. 3. Main parts of the mentioned contact (1 – base board; 2 – supporting holders; 3 – pressure springs; 4 – saddle contacts; 5 – bus-bar that fits into the saddle)

A. Material of the parts used:

- base-board is made of copper,
- supporting holders are made of steel,
- pressure springs are made of steel,
- saddle contacts are made of polished copper,
- bus-bar is made of copper.

TABLE II. MATERIAL PROPERTIES OF PARTICULAR PARTS FOR THERMAL ANALYSIS

Parameter / material	**Baseboard; Saddle contacts; buss-bar; (Cu_1)**	**Supporting holder; Pressure spring (Fe)**	**Impurity (inhomog.)**
$\rho_{20°C}$ [kg·m^{-3}]	8960	7870	2400
$c_{20°C}$ [J·kg^{-1}·K^{-1}]	385	450	1085
$\lambda_{20°C}$ [W·m^{-1}·K^{-1}]	401	76	30
$\rho_{el,20°C}$ [Ω·m]	$1{,}7\cdot10^{-8}$	$9{,}7\cdot10^{-8}$	0,002

Where: $\rho_{20°C}$ specific volume density at 20°C,

$c_{20°C}$ specific heat capacity at 20°C,

$\lambda_{20°C}$ thermal conductivity at 20°C,

$\rho_{el,20°C}$ electric resistivity at 20°C.

B. Dimensional parameters of impurity for simulation

An impurity thickness of 1 mm was used to create the impurity model, although in reality it can only reach a thickness of 10^{-8} m to simplify meshing. The electro-thermal physical parameters of this layer were adjusted accordingly.

C. Geometrical parameters of electrical contact:

- height of one contact: 75 mm,
- width of one contact: 15 mm,
- impurity thickness: 1 mm,
- area of one contact: 1125 mm^2,
- total area of impurity: 4860 mm^2.

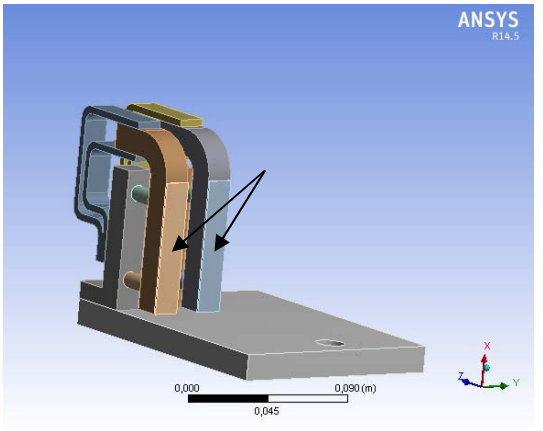

Fig. 4. View on the areas, that were considered as impurities

D. Thermal surface losses

When modeling, one must also consider the location where the contact is used. For the calculation, it was necessary to determine the boundary conditions, i.e. the wall surfaces from which heat transfer into the environment is considered. For the upper contact surfaces, the heat transfer coefficient α was chosen to be 4 W·m^{-2}·K^{-1} and for the side and lower walls 3 W·m^{-2}·K^{-1} (for considering the location of the contacts in a horizontal position).

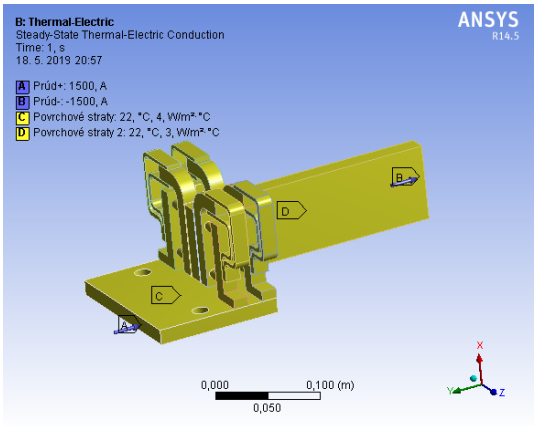

Fig. 5. Place definition of boundary conditions at each point of contact

IV. Calculation of Contact Resistance

If one presses two metal materials on each other by force F_k, then the specific type of joint contact is made. If we observed the place of this contact under the microscope, we would find that even on technically flat surfaces there is no contact on the whole surface, but only in a certain number of microscopic surfaces, which is given by microscopic surface irregularities (Fig. 6). This number is random. The size and the number of microplates also depend on the mechanical properties of the materials and the contact force F_k. The formation of contact in the micro-surfaces causes both the deformation of the nozzles (their elongation) and the reduction of the cross-section through which the current passes. This increases the electrical resistance of the contact point (straits) R_u. [1]

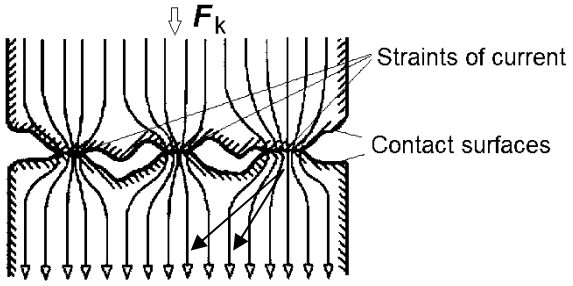

Fig. 6. Display of areas on which impurities were considered

If it is assumed that the contact is made up of n equal areas and there is no mutual interaction of the current field, the resulting strait resistance will be given by:

$$R_u = \frac{\rho}{2r_0} \ [\Omega] \tag{1}$$

The size of the contact areas depends on the properties of the contacts (shape and material) and also on the pressure force F_k. The type of material deformation that occurs at the point of contact is critical. According to the shape of contacts and mutual geometric arrangement it is possible to recognize:

- point contact (junction)
- line contact (junction)
- surface contact (junction)

Point contact is achieved if the spherical surfaces, or the spherical surface with a flat surface, or two crossed cylinders touch. *Line contact* is formed when the cylinder contacts the plane along the body surface. *Surface contact* is obtained by contact of two contacts with flat surfaces.

The radius of the contact surfaces depends on the type of deformation. In the arrangement of a sphere and a plane of the same material, the elastic deformation shall be given by the formula:

$$r_0 = 1{,}11\sqrt[3]{\frac{F_k r_k}{E}} \ [\text{m}] \tag{2}$$

In this case, there were used equations (1) and (2) as well as an analysis referred in [1], where for this case the radius of the circular surfaces is $r_0 = 0.037$ m. By substituting the values, the resistance of the strait is $R_u = 1{,}497 \cdot 10^{-7}$ Ω/m. If the total contact resistance consisted only of this component, the thermal analysis (distribution of temperature field) of the contact is shown in the figure Fig. 7.

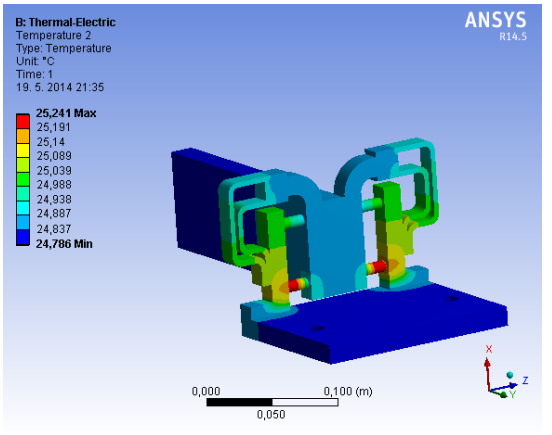

Fig. 7. Temperature field of the 1 pair of saddle contacts, considering only the strait resistivity

For a more precise analysis, several factors that affect the accuracy of the contact resistance determination should be taken into account, so the following equation will be used in the next analysis:

$$R_S = \frac{k_n}{\left(\frac{F_k}{F_1}\right)^m} \ [\Omega] \tag{3}$$

Where $F_1 = 1$ N and F_k is contact pressure force.

The coefficient k_n includes the properties of the material itself, the properties of the layers and the contact point conditions. For these reasons, it varies in size, and varies widely for some materials. The exponent m affects the most important property and it is the type of contact:

- point contact (junction) $m = 0{,}5$,
- line contact (junction) $m = 0{,}5$ to $0{,}7$,
- surface contact (junction) $m = 0{,}6$ to 1.

For copper and silver contacts, the contact resistance dependence on pressure force is shown in Fig. 8. Coefficient k acquires values of $k_{Cu} = (15 \text{ to } 400)\cdot 10^{-4}$ Ω, $k_{Ag} = (3{,}8 \text{ to } 12)\cdot 10^{-4}$ Ω, lower value applies to clean surface and higher to corroded surface.

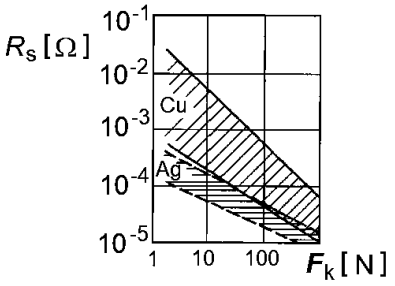

Fig. 8. Contact resistance dependence on pressure contact force F_k for Cu and Ag [1]

For determining the resulting contact resistance, it is also necessary to consider the resistance of the foreign layers. This is included in the coefficient k_n in equation (3). If it is assumed that due to the pressure springs, the resulting contact force $F_k = 200$ N, and the contacts are degreased and polished, the resulting resistance is obtained as $R_s = 0{,}002$ Ω/m.

V. Temperature Field Distribution Solution of 500 A Electrical Contact

When analyzing the temperature field, it was necessary to find out which places were most stressed and therefore it was necessary to determine the minimum contact area and thus the number of saddles. Individual alternatives using of 1-, 2- and 3-saddle contacts are shown in the following figures.

A. Analysis of 1 pair of saddle contacts

When using only one pair of saddle contacts, the contact point is heated to 482.03 °C. The exact temperature distribution is shown in the figure Fig. 9.

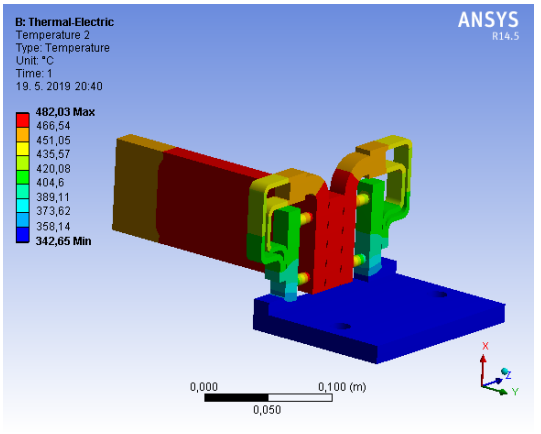

Fig. 9. Temperature field distribution of 1 pair of saddle contacts

With a doubled increase in surface heat loss (by a forced convection), the point of contact was cooled to temperature of 278.65 °C (Fig. 10).

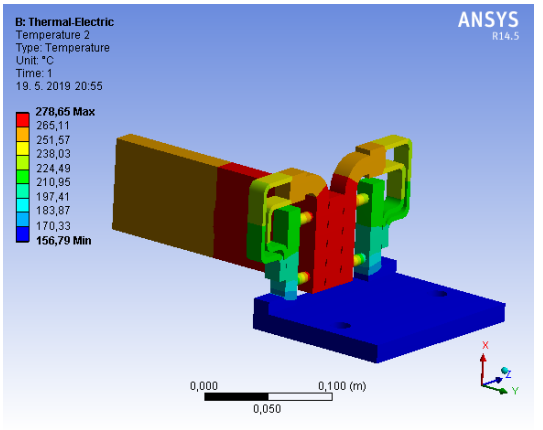

Fig. 10. Temperature field distribution of 1 pair of saddle contacts after applying forced cooling

In this solution of lowering the temperature, it is necessary to use further investments in cooling device for lowering the ambient temperature. A more economical method is to use another pair of saddle contacts as it follows.

B. Analysis of 2 pairs of saddle contacts

If 2 pairs of saddle contacts are used, the contact temperature rapidly decreases to 176.61 °C (Fig. 11).

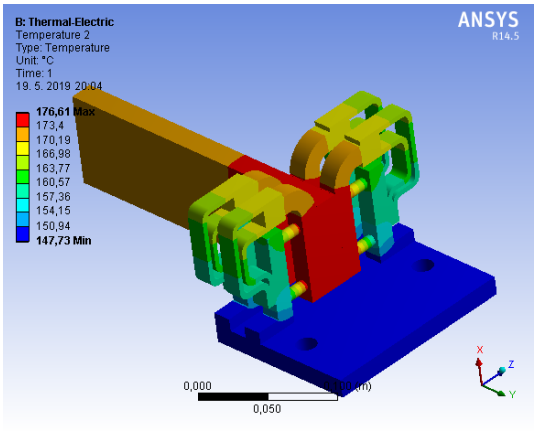

Fig. 11. Temperature field distribution of 2 pairs of saddle contacts

When using a cooling fan that causes doubled heat dissipation, the temperature is reduced to 105.54 °C (Fig. 12), but it still does not confirm the temperature condition.

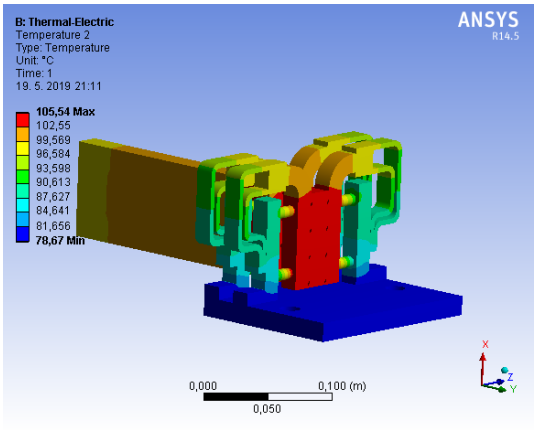

Fig. 12. Temperature field distribution of 2 pairs of saddle contacts after applying forced cooling

C. *Analysis of 3 pairs of saddle contacts*

When using 3 pairs of saddle contacts, the contact area is 9 000 mm^2. The highest temperature that was reached was at the point of contact, 64.363 °C (Fig. 13), that confirm the main condition, and therefore it is not necessary to add supplementary cooling device.

This analysis validated the recommendation of the producer of that type of contacts, that for the 500 A applications, it is necessary to use 3 pairs of saddle contacts instead of 2 or just 1 pair.

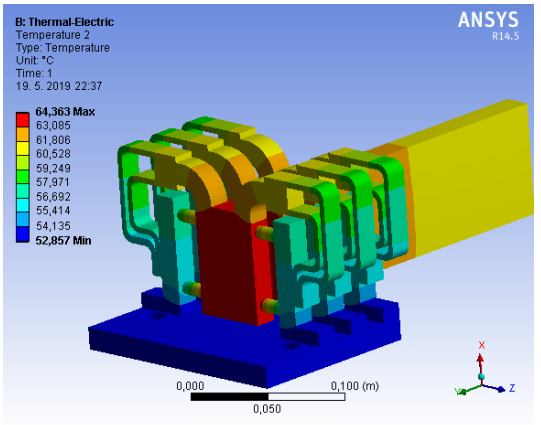

Fig. 13. Temperature field distribution of 3 pairs of saddle contacts

VI. Conclusion

The aim of this paper was to present an analysis of the temperature field distribution of high-current electrical contacts, which was realized in the ANSYS environment. It is apparent from the results compared that by utilizing a plurality of saddle contacts and thus increasing the contact area, the contact resistance of the contact layer is reduced, thereby reducing Joule losses and hence the temperature of the contact itself. Thus, the total current flows through a larger area and less stresses some of the bottlenecks that would overheat. Another alternative to increasing the contact area is to change the material, to modify the material as well as to increase the contact force of the contacts, or to add additional cooling (active, passive).

Acknowledgment

The Ministry of Education, Science, Research and Sport of the Slovak Republic and the Slovak Academy of Sciences under the contract no. VEGA 1/0372/18 supported this work.

References

[1] O. Havelka, et. al., "*Elektrické prístroje*", Praha SNTL 1985. 436 pp.

[2] Druseidt elektrotechnik,"*Product information 02/2011*", Available at: < http://www.druseidt.de/pdf/0211eng.pdf >.

[3] Druseidt elektrotechnik, "*Contact-Systems and Accessories for Anodising and Electroplating Equipment*", 2000, Available at: < http://www.druseidt.de/pdf/kat3eng.pdf >.

[4] T. Poľák, D. Medveď, "*Teplotná analýza elektrických kontaktov vysokoprúdových zariadení*". In: Electrical Engineering and Informatics 5: Proceeding of the FEI of the TU of Košice. Košice: TU, 2014. pp. 206-209. ISBN 978-80-553-1704-5.

[5] P. Liptai, et. al., "*Check measurements of magnetic flux density: Equipment design and the determination of the confidence interval for EFA 300 measuring devices*", In: Measurement. Vol. 111 (2017), p. 51-59. ISSN 0263-2241.

[6] L. Misencik, D. Medved, "*Design of Dry Transformer Cooling*". In: Elektroenergetika. Vol. 6, No. 3 (2013), p. 28-31. ISSN 1337-6756.

[7] M. Pavlík, et. al., "*The impact of electromagnetic radiation on the degradation of magnetic ferrofluids*", In: Archives of Electrical Engineering. Vol. 66, no. 2 (2017), p. 361-369. ISSN 1427-4221.

[8] J. Zbojovský, M. Pavlík, "*Calculating the shielding effectiveness of materials based on the simulation of electromagnetic field*", In: Elektroenergetika 2017. Košice: TU, 2017 p. 369-372. ISBN 978-80-553-3195-9.

[9] J. Kurimsky, R. Cimbala, I. Kolcunova, "*Multi-scale decomposition for partial discharge analysis*", In: Przeglad Elektrotechniczny. Vol. 84, no. 9 (2008), p. 169-173. ISSN 0033-2097.

[10] D. Rot, J. Jirinec, J. Kozeny, A. Podhrazky, J. Hajek, S. Jirinec, "*Induction system for hardening of small parts*". In Proceedings of the 2018 19th International Scientific Conference on Electric Power Engineering (EPE). Piscataway: IEEE, 2018, p. 277-282. ISBN: 978-1-5386-4612-0, ISSN: 2376-5623.

[11] D. Rot, J. Kozeny, S. Jirinec, J. Jirinec, A. Podhrazky, I. Poznyak, "*Induction melting of aluminium oxide in the cold crucible*", In: 18th International Scientific Conference on Electric Power Engineering (EPE) 2017, pp 1-4, DOI: 10.1109/EPE.2017.7967281.

[12] R. Cimbala, J. Kiraly, M. German-Sobek, S. Bucko, J. Kurimsky, J. Dzmura, "*Polarization Phenomena in Magnetic Liquids*", Chemicke listy 109, No. 2 (2015), 117–124. ISSN 2336-7202.

[13] J. Petráš, J. Kurimský, J. Balogh, R. Cimbala, J. Džmura, B. Dolník, I. Kolcunová, "*Thermally Stimulated Acoustic Energy Shift in Transformer Oil*", In: Acta Acoustica United with Acustica, Vol. 102 Issue: 1 Pages: 16-22, ISSN 1610-1928.

[14] M. Pavlík, et. al., "*Measuring of Dependence of Shielding Effectiveness of Wet Materials on the Frequency of Electromagnetic Field in the High Frequency Range*", In: Acta Electrotechnica et Informatica. Vol. 13, No. 3 (2013), p. 12-16. ISSN 1335-8243.

[15] J. Zbojovsky, M. Pavlik, Z. Conka, L. Kruzelak, M. Kosterec, "*Influence of shielding paint on the combination of building materials for evaluation of shielding effectiveness*". In: EPE 2018. Brno: Univ. of Technology, 2018, pp. 324-327. ISBN 978-1-5386-4611-3.

[16] V. Volokhin, I. Diahovchenko, V. Kurochkina, M. Kanálik, "*The influence of nonsinusoidal supply voltage on the amount of power consumption and electricity meter readings*", In: Energetika. Vol. 63, no. 1 (2017), p. 1-7. ISSN 0235-7208.

[17] Z. Eleschova, A. Belan, B. Cintula, B. Bendik, "*Smart grids analysis – View of the transmission systems voltage stability*", In EPE 2018. Brno: Univ. of Techn., 2018, pp. 37-42. ISBN 978-1-5386-4612-0.

[18] D. Kapral, P. Bracinik, M. Roch, M. Hoger, "*Optimization of distribution network operation based on data from smart metering systems*", Electrical Engineering, Vol. 99, Issue 4, Springer, New York, USA, 2017, December, pp: 1417-1428, ISSN 0948-7921.

[19] M. Spes, L. Bena, M. Kosterec, M. Marton, "*Determining the current capacity of transmission lines based on ambient conditions*", In: Journal of Energy Technology. Vol. 10, no. 2 (2017), p. 61-69. ISSN 1855-5748.

[20] M. Spes, L. Bena, M. Mikita, M. Marton, H. Wachta, "*Possibilities of increasing transmission capacity overhead lines*", In: Acta Elect. et Inf. Vol. 16, No. 3 (2016), p. 20-25. ISSN 1335-8243.

[21] M. Kmec, Ľ. Beňa, L. Lisoň, "*Influence of parallel line mutual coupling on distance relay operation*", In: Acta Electrotechnica et Informatica. Vol. 14, No. 4 (2014), p. 35-41. ISSN 1335-8243.

[22] J. Dzmura, J. Petras, J. Balogh, J. Kurimsky, R. Cimbala, I. Kolcunova, B. Dolnik, M. Kolcun, "*Separation of solid particles from flowing,gases by AC high voltage*", In: Journal of electrostatics, Vol. 88, Elsevier Science BV, 2017, pp. 158-164, ISSN: 0304-3886.

[23] M. Tesarova, R. Vykuka, "*Impact of Distributed Generation on Power Flows Along Parallelly Operated MV Feeders*", DOI: 10.1109/EEEIC.2018.8493640.

[24] K. Nohac, M. Tesarova, L. Nohacova, J. Veleba, V. Majer, "*Utilization of Events Measured by WAMS-BIOZE-Detector for System Voltage Stability Evaluation*", IFAC-PapersOnLine, Volume 49, Issue 27, 2016, pp 364-369, DOI: 10.1016/j.ifacol.2016.10.747.

[25] M. Kolcun, M. Kornatka, A. Gawlak, Z. Conka, „Benchmarking the reliability of medium-voltage lines", In: Journal of electrical engineering, Vol. 68, Issue: 3, Pages: 212-215, 2017, DOI: 10.1515/jee-2017-0031, ISSN: 1335-3632.